Proceedings of the Sixth International Conference on
Railway Technology: Research, Development and Maintenance
Edited by: J. Pombo
Civil-Comp Conferences, Volume 7, Paper 16.5
Civil-Comp Press, Edinburgh, United Kingdom, 2024
ISSN: 2753-3239, doi: 10.4203/ccc.7.16.5

Recursive Radial Basis Neural Network-Based Model for Predictive Control of Maglev Vehicles

W. Zhang,[1,2] H. Wu,[1,2] S. Fu,[3,4] X. Liang[3,4] and X. Zeng[1,2]

[1]School of Future Technology
University of Chinese Academy of Sciences, Beijing, China
[2]Key Laboratory for Mechanics in Fluid Solid Coupling Systems
Institute of Mechanics, Chinese Academy of Sciences, Beijing, China
[3]Qingdao Sifang Co., Ltd., CRRC, China
[4]State Key Laboratory, High-Speed Maglev Transportation Technology
Qingdao, China

Abstract

The levitation control system plays a pivotal role in governing the intricate aerodynamic load-vehicle-rail coupling vibration process, a crucial determinant of vehicle stability. As speed escalates, the impact of aerodynamic load and vehicle-rail coupling on levitation stability becomes increasingly undeniable. Conventional proportional-integral-derivative (PID) controllers, while effective in simpler environments, exhibit diminished performance within the complexities of high-speed mechanical systems. To address the pressing need for accurate prediction of non-stationary aerodynamic performance in high-speed maglev vehicles, we propose a load prediction model based on the Recursive Radial Basis Function Neural Network (RRBF). This model, leveraging recursive history information in loop neurons, offers dynamic memory capabilities, thus enhancing its learning of temporal patterns. The RRBF network predicts real-time aerodynamic load based on time series states. Simultaneously, we introduce a robust Nonlinear Model Predictive Controller (NMPC), designed to consider the physical constraints of the chopper and the influence of aerodynamic loads on the model's future dynamic behaviours. The algorithm ensures optimal roll optimization within finite time, accounting for constraints. Stability assessments of an electromagnet under non-stationary aerodynamic loads and random track irregularities are conducted through a minimum levitation unit dynamics-control co-simulation model. Results highlight the RRBF's precise identification of aerodynamic loads. Moreover, the Recursive Radial Basis Function Neural Network-based Model Predictive Controller (RMPC) demonstrates superiority over the PID method, showcasing exceptional disturbance resistance and making it more suitable for high-speed maglev levitation control.

Keywords: Maglev vehicle, neural network, nonlinear dynamics, model predictive control, state constraints, recursive radial basis function

1 Introduction

As industrial technology continues to advance, high-speed maglev systems have garnered increasing attention as a vital component of modern transportation. The field of high-speed magnetic levitation encompasses various principles, including electrodynamic EDS, high-temperature superconducting HTS, and electromagnetic EMS levitation. In this paper, we specifically concentrate on the commercially operational electromagnetic (EMS) scheme. The levitation system employed in EMS high-speed magnetic levitation vehicles exhibits instability in an open loop. To achieve stable levitation, feedback control becomes imperative [1]. Consequently, the stability, safety, and comfort of the vehicle are intricately linked to the efficacy of the control behaviours implemented.

In recent years, diverse control methods have been explored for achieving tracking control in nonlinear levitation systems. WANG [2] delved into the coupled response of high-speed Maglev vehicles and bridges, employing a proportional-integral-derivative (PID) control mechanism. Yau [3], on the other hand, leveraged a back-propagation neural network to dynamically adjust PI controller parameters in real-time response to state changes. While these advanced control methodologies partially address the feedback control challenge, the escalating speed introduces heightened effects of aerodynamic loads and vehicle-rail coupling. Inadequate feedback control, particularly within the PID scheme relying on equilibrium point linearization [4], results in performance degradation, emphasizing the critical need for more robust levitation control algorithms suited for aerodynamic loads. Enter the Model Predictive Controller (MPC), a control scheme resilient to model nonlinearity and uncertainty [5]. This algorithm predicts an approximate future response based on the dynamical model, current inputs, and predicted disturbances. By formulating a constrained optimization problem in a finite time domain, MPC seeks to obtain the optimal control sequence considering the present state. This approach, accounting for both the present state and the impact of disturbances on the future state, endows MPC with feed-forward rejection capabilities against disturbances, showcasing superior robustness compared to the PID scheme.

Undoubtedly, the efficacy of the Model Predictive Controller (MPC) method hinges on prediction accuracy, and any model mismatch can lead to inappropriate control actions, resulting in a degradation of control performance [6]. In real-world environments, where electromagnetic force nonlinearity and disturbance uncertainty are inevitable, various coping strategies have been proposed to tackle the effects of system nonlinearity and time-varying disturbances. Shen [7] employed a Kalman filter to meticulously observe state changes in a vehicle under track coupling, while Sun [8] adeptly utilized an adaptive repetitive learning filter to learn and predict periodic disturbances. Sun [9] introduced an adaptive radial basis neural network for online prediction and feedback suppression of the time-varying mass in the maglev system. Model Predictive Control algorithms inherently exhibit high resistance to interference, and the radial basis neural network (RBF), known for its simplicity and

high accuracy, presents itself as an invaluable asset in high-speed magnetic levitation control. The fusion of MPC and RBF emerges as a judicious choice.

In this paper, we meticulously design a Nonlinear Model Predictive Controller (NMPC) tailored for high-speed magnetic levitation, emphasizing heightened robustness. To further elevate our approach, we integrate a Recursive Radial Basis Function Neural Network (RRBF) for real-time prediction of aerodynamic loads. Using the TR08 high-speed maglev minimum levitation unit dynamics and control co-simulation model [10,11], we conduct a comprehensive comparison of the levitation control performances between PID and Recursive Radial Basis Function Neural Network-based Model Predictive Controller (RMPC) under various conditions, including aerodynamic loads, track disturbances, and random track irregularities, coupled with non-stationary aerodynamic loads. The study unequivocally demonstrates that the designed RMPC excels in disturbance compensation, establishing its suitability for high-speed magnetic levitation control in complex nonlinear environments.

2 Dynamic model

Through the levitation frame decoupling test [12], it can be found that the levitation system can be degraded to a single electromagnet control problem. The coupling effect between each electromagnet is partially decoupled, and the single electromagnet characteristic has universality and generality. Therefore, this paper is based on the single electromagnet structure to develop the analysis. Figure 1 shows the structure of the minimum levitation unit with a single electromagnet.

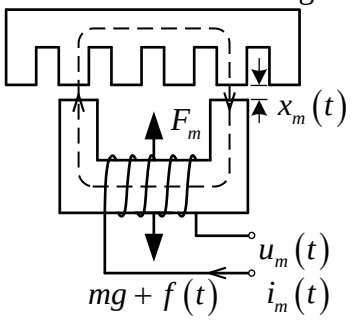

Figure 1 The structure of the minimum electromagnet unit

Neglecting the influence of magnetoresistance between the levitation gaps as well as leakage magnetism between the electromagnet windings, a set of dynamic equation for the electromagnetic single electromagnet levitation system can be obtained. The vertical equation can be further simplified due to the presence of current saturation in the actual controller:

$$m\ddot{x}(t) = -\frac{\mu_0 N^2 A}{4m}\left\{\frac{\mathrm{sat}\left[i(t)\right]}{x(t)}\right\}^2 + mg + f_d(t) \tag{1}$$

$$\mathrm{sat}\left[i(t)\right] = \begin{cases} i_{\max}, i > i_{\max} \\ i(t), 0 \le i \le i_{\max} \end{cases}$$

where m is the mass of the electromagnet, $x(t)$ is the levitation gap, N is the number of turns of the electromagnet coil, A is the area of the magnetic poles, $i(t)$ is the current of the electromagnet coil, μ_0 is the air permeability, f_d is the external disturbance, and g is the gravitational acceleration.

2 Controller design

In this section, a high-speed maglev nonlinear model predictive controller and an aerodynamic load RRBF predictor are designed.

2.1 Model predictive controller

The nonlinear model predictive controller mainly consists of a dynamic predictive model, an online rolling optimization algorithm and a feedback correction loop. The algorithm will, at each moment, compute online a constrained optimization problem in a finite time domain based on the current state and the predicted disturbances. The next moment will update the measured state and repeat the above steps to form a rolling optimization.

As shown in Figure 2, at each sampling step, first the RRBF predicts the unmeasurable aerodynamic loads in real time based on the current measurable state. Then the prediction model of MPC is corrected to enable the dynamic prediction model to have strong future prediction capability. The rolling optimizer then solves the open-loop optimization problem in the finite time domain in real time by combining the control quantities, state constraints and cost functions. Finally, the first control quantity of the optimal sequence is imported into the controlled system. Considering the error between the prediction and the real model, the feedback session will delay the calculation of the error between the current prediction and the real state, and compensate the next prediction quantity to further improve the prediction ability of the dynamic model.

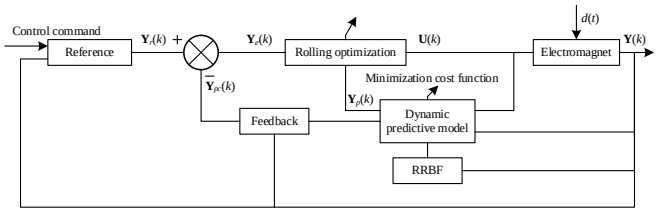

Figure 2 Schematic diagram of RMPC

Taking into account that the sensors can measure the gap state in real time, the non-singular transformation of the coordinates of the nonlinear system into a controllable linear system is performed by introducing a new control quantity w:

$$w(t)=\left(\frac{i(t)}{x(t)}\right)^2 \tag{2}$$

The electromagnetic force is proportional to the square of the current, so the electromagnetic force is sensitive to current changes. In order to prevent sudden current changes from adversely affecting the suspension stability, the discrete

equation of state is expanded for the measured current (control quantity) state. The discrete state equations for the expansion of the measured current can be obtained:

$$\begin{cases} \boldsymbol{\xi}(k+1) = \mathbf{A_k}\boldsymbol{\xi}(k) + \mathbf{B_k}\Delta\mathbf{W}(k) + \mathbf{F}_k(t) \\ \boldsymbol{\eta}(k) = \mathbf{C_k}\boldsymbol{\xi}(k) \end{cases} \tag{3}$$

where

$$\begin{cases} \mathbf{A_k} = \begin{bmatrix} \mathbf{A_c} & \mathbf{B_c} \\ \mathbf{0}_{m\times n} & \mathbf{I}_m \end{bmatrix} \\ \mathbf{B_k} = \begin{bmatrix} \mathbf{B_c} \\ \mathbf{I}_m \end{bmatrix} \\ \mathbf{F_k} = \begin{bmatrix} \mathbf{F}_c(t) \\ \mathbf{0} \end{bmatrix} \\ \mathbf{C_k} = \begin{bmatrix} \mathbf{C} & \mathbf{0} \end{bmatrix} \end{cases} \quad \begin{cases} \mathbf{A}_c = \begin{bmatrix} 1 & T_s \\ 0 & 1 \end{bmatrix} \\ \mathbf{B}_c = \begin{bmatrix} 0 \\ -\dfrac{\mu_0 N^2 A}{4m} T_s \end{bmatrix} \\ \mathbf{C}_c = \begin{bmatrix} 1 & 0 \end{bmatrix} \\ \mathbf{F}_c = \begin{bmatrix} 0 \\ T_s\left[\dfrac{f_d(t)}{m} + g - \ddot{h}(t)\right] \end{bmatrix} \end{cases}$$

$\boldsymbol{\xi}(k)$ is the expanded state variable, $\boldsymbol{\xi}(k)=[\mathbf{X}(k)\ \mathbf{W}(k\text{-}1)]^{\mathrm{T}}$; $\mathbf{W}(k\text{-}1)$ is the measured control input; $\Delta\mathbf{W}(k)$ is the control input increment, $\boldsymbol{\eta}(k)$ is the expanded output, $\mathbf{A}_k$ is the expanded state matrix, $\mathbf{B}_k$ is the expanded control matrix, $\mathbf{C}_k$ is the expanded output matrix, and $\mathbf{F}_k$ is the expanded disturbance matrix. $\mathbf{X}(t)$ is the state variable of the system, $w(t)$ is the constructed feedback control input, $\mathbf{Y}(t)$ is the output of the system, $\mathbf{A}_c$ is the state matrix, $\mathbf{B}_c$ is the control matrix, $\mathbf{C}_c$ is the output matrix, $\mathbf{F}_c$ is the perturbation matrix, f_d is the measurable disturbances, x_1 is the levitation gaps and x_2 denotes the velocity of the electromagnet.

Assuming that the prediction space is N_p, the control space is N_c, the disturbance space is N_f, and $N_c<N_f=N_p$, the magnitude of the control quantity outside the control space is kept constant. To ensure that the levitation gap tracks the nominal gap accurately and smoothly. In addition, to avoid sudden changes in current during the control process. The finite time domain optimal control cost function considers the effects of the prediction output error and the control quantity changes:

$$\min_{\Delta\mathbf{U}(t)} J\left(\boldsymbol{\xi}(t), \Delta\mathbf{W}(t)\right) = \sum_{i=1}^{N_p} \left\| \boldsymbol{\eta}(k+i|k) - \boldsymbol{\eta}_{ref}(k+i|k) \right\|_{\mathbf{Q}_e}^2 + \sum_{i=1}^{N_c} \left\| \Delta\mathbf{W}(k+i-1|k) \right\|_{\mathbf{R}_e}^2 \tag{4}$$

s.t.

$$\boldsymbol{\xi}_{\min} \le \boldsymbol{\xi}_{k,t} \le \boldsymbol{\xi}_{\max},\ k = t, \cdots, t+N_p$$

$$\mathbf{U}_{\min} \le \mathbf{U}(t) \le \mathbf{U}_{\max},\ k = t, \cdots, t+N_p$$

$$\Delta\mathbf{W}(k) = \mathbf{W}(k) - \mathbf{W}(k-1)$$

By considering the model predictive control rolling optimization structure, the first element of the optimal control sequence is fed into the control system at each moment in time.

$$u(t) = x_1(t)\left\{\begin{bmatrix}1 & 0 & \cdots & 0\end{bmatrix}\Delta\mathbf{U}(t) + w(t-1)\right\}^{\frac{1}{2}} \tag{5}$$

2.2 Recursive radial basis neural network load predictor

It is difficult to measure or accurately predict the time-varying external loads of a magnetic levitation vehicle during its actual operation. As the vehicle speed increases, the external load represented by the aerodynamic load increases significantly, and its effect on the levitation stability cannot be ignored. To solve this problem, this paper introduces a radial basis neural network predictor [13]. RBF is a forward neural network, and its structure is shown in Figure 3. The network consists of an input layer, a single hidden layer and an output layer. The hidden layer and the output layer are connected linearly. Therefore, compared to the multilayer perceptron (MLP), the RBF training and running is faster due to the simple and lightweight structure without lengthy loop computation. Gaussian basis function has better prediction effect. And the output of RBF neural network can be expressed as:

$$F_p = \sum_{i=1}^{N} w_i \cdot \varphi\left(\left\|\boldsymbol{\xi} - c_i\right\|\right) = \sum_{i=1}^{N} w_i \cdot \exp\left(-\frac{\left\|\boldsymbol{\xi} - c_i\right\|^2}{2d_i^2}\right) \tag{6}$$

where $\boldsymbol{\xi}(k)$ is the input vector, $\mathbf{F}_p$ is the prediction vector. The designed network has N hidden layers, the hidden layer output is φ, the weights of the hidden and output layers are w_i, c_i is the centre of the hidden layer Gaussian function, and d_i is the Gaussian function width.

Traditional RBF architectures do not consider the past state of the input data. In general, temporal memory in neural network architectures can be represented either spatially or dynamically. The spatial method converts temporal information into spatial information [14]. The dynamic method stores historical information implicitly inside the network through recursive neurons [15]. In this paper, by introducing recurrent loop neurons with historical information, RRBF can have a dynamic memory capability for time delays. The scheme of the RRBF neural network is shown in Figure 4. Due to the difference in the input unit system, the network cannot learn the data equally. Therefore, in order to learn the information equally and comprehensively, the effect of the unit system is eliminated using a normalization method based on the maximum and minimum values. In addition, in order to enhance the network's learning of the current state, a forgetting factor is introduced. The state memory is gradually forgotten with the continuous input of time series until it is replaced by new data. Thus, the proposed new RRBF network can be expressed as:

$$F_p = f\left(\boldsymbol{\xi}(t), \gamma^1 \cdot \boldsymbol{\xi}(t - t_0), \gamma^2 \cdot \boldsymbol{\xi}(t - 2 \cdot t_0), \ldots, \gamma^{n_k} \cdot \boldsymbol{\xi}(t - n_k \cdot t_0)\right) \tag{7}$$

where γ is the forgetting factor, t_0 is the delayed memory time, n_k is the number of delayed memory neurons, and $f(t)$ is the RBF expression.

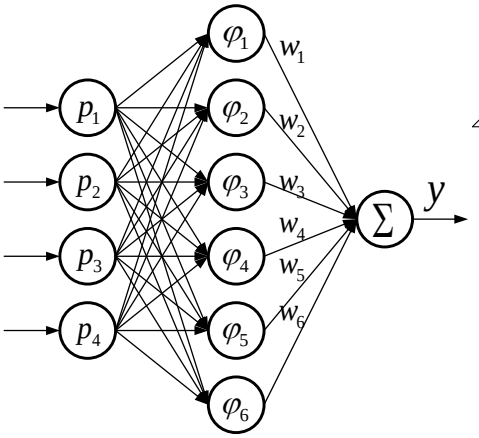

Figure 3 RBF network architecture

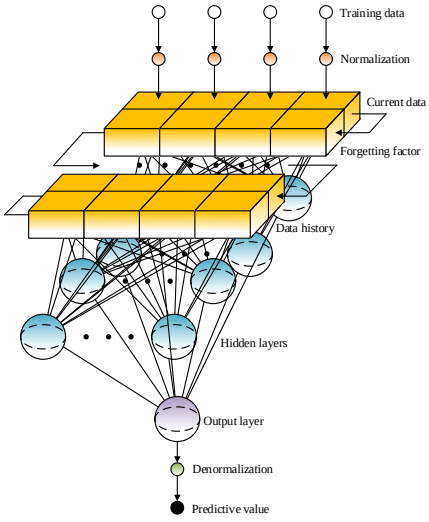

Figure 4 RRBF network architecture

Centres and widths are determined using unsupervised learning: The strength of RBF neural networks lies in the local representation of the N-dimensional space. In this paper, the K-MEANS clustering algorithm is used to determine the RBF centres. The maximum cluster width of each family is then calculated according to the KNN algorithm. The supervised learning is used to determine the weights between the hidden and output layers. Specifically, an adaptive gradient descent algorithm with a small batch training sets (Batch-Adam) is used. The network input vector includes the actual levitation gap error, gap change velocity, gap change acceleration and measured current. And the network output is the real-time aerodynamic load. By learning the simulation results of lift-vehicle-rail coupling maglev dynamic, the prediction results of loads are shown in Figure 5, 6 and Table 1.

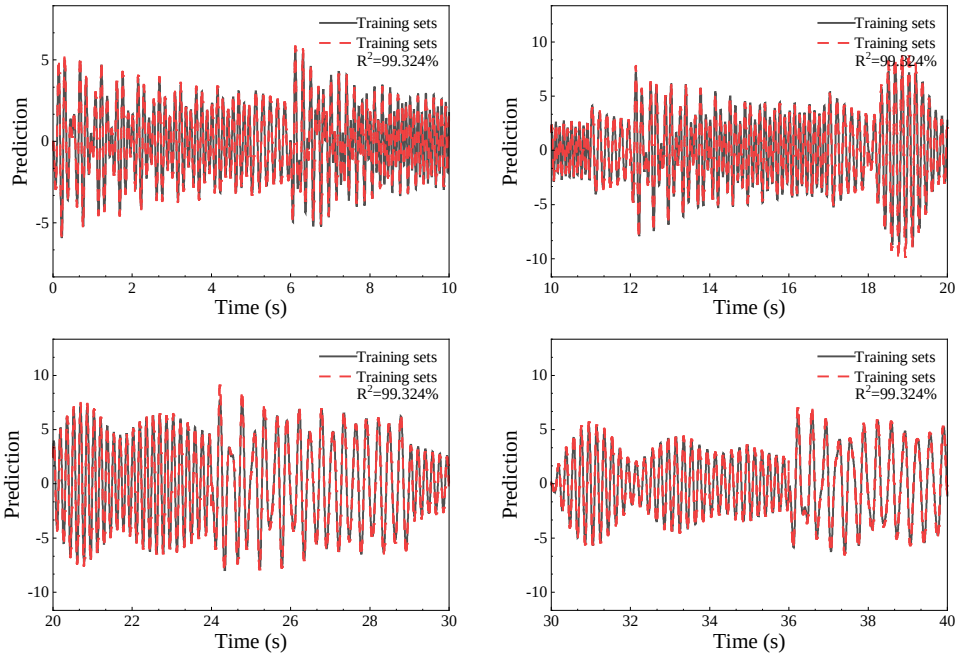

Figure 5 RRBF prediction results for the training sets

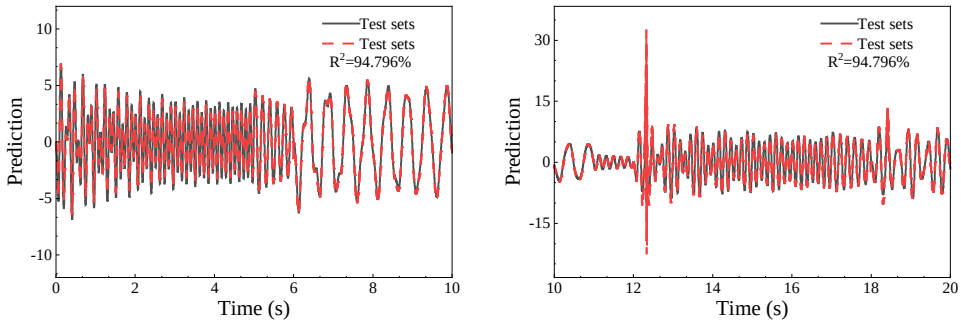

Figure 6 RRBF prediction results for the test sets

Load prediction	R^2	MAE
Training sets	99.324%	0.18382
Test sets	94.796%	0.36455

Table.1 Comparison of RRBF prediction results

The individual network structure of this network is 4-60-1, with a forgetting factor γ =0.9, a delayed memory time t_0=0.01s, and a number of delayed memory neurons n_k =10. Analysing Figure 5, 6 and Table 1 it can be found that R^2 = 99.324% and MAE = 0.18382 for training sets and R^2 = 94.796% and MAE = 0.36455 for testing sets. The designed RRBF network can accurately predict the loads for 0.01s.

3 Simulation results

The goal of levitation control of maglev vehicles is to keep the levitation gap of electromagnet stable near the reference gap (10mm) with as little fluctuation. The initial/maximum levitation gap is 20mm, and the minimum levitation gap is 0 mm. Based on the TR08 high-speed maglev minimum levitation unit dynamics and control co-simulation model [10,11]. The control performance of the PID and RMPC controllers are compared. The controller parameters are shown: N_p=5, N_c=3, N_f=3, Q=1×10^{19}, R=1, electromagnet mass 603kg, levitation frame mass 660kg, body mass 490kg, first suspension stiffness 2×10^7 N/m, second suspension stiffness 2.0×10^5 N/m.

3.1 Under harmonic aerodynamic load conditions

CFD simulations of a 600km/h maglev vehicle revealed that the aerodynamic lift fluctuations are significant at high speeds and that the aerodynamic lift can reach up to 40% of the vehicle weight [16]. Thus, the simulation is divided as:

Group1: $F_1 = 0.20 \cdot mg\left[1+\sin\left(2\pi \cdot 2t\right)\right]$; Group2: $F_2 = 0.20 \cdot mg\left[1+\sin\left(2\pi \cdot 4t\right)\right]$; Group3: $F_3 = 0.20 \cdot mg\left[1+\sin\left(2\pi \cdot 6t\right)\right]$; Group4: $F_4 = 0.20 \cdot mg\left[1+\sin\left(2\pi \cdot 8t\right)\right]$

The levitation gap versus time history curves are shown in Figure 7. Analysing the red curve reveals that the electromagnet under the PID controller encounters a track collision problem under 4 Hz harmonic lift (reach the minimum levitation gap). The

control performance of the PID controller decreases, and the electromagnet levitation gap fluctuates significantly around the nominal gap of 10mm. The gap fluctuation is greater than 2mm with some offset and divergence tendency. The PID controller has limited anti-interference capability. RMPC controller has a maximum deviation of 0.8mm gap error under 2Hz load. In addition, the maximum deviation is 1.0mm at 4Hz, 3.0mm at 6Hz, and 0.8mm at 8Hz. Therefore, the RMPC can effectively inhibit vibration caused by high-speed aerodynamic loads. By solving the rail collision problem, the anti-interference ability and robustness of RMPC are better than that of PID controller.

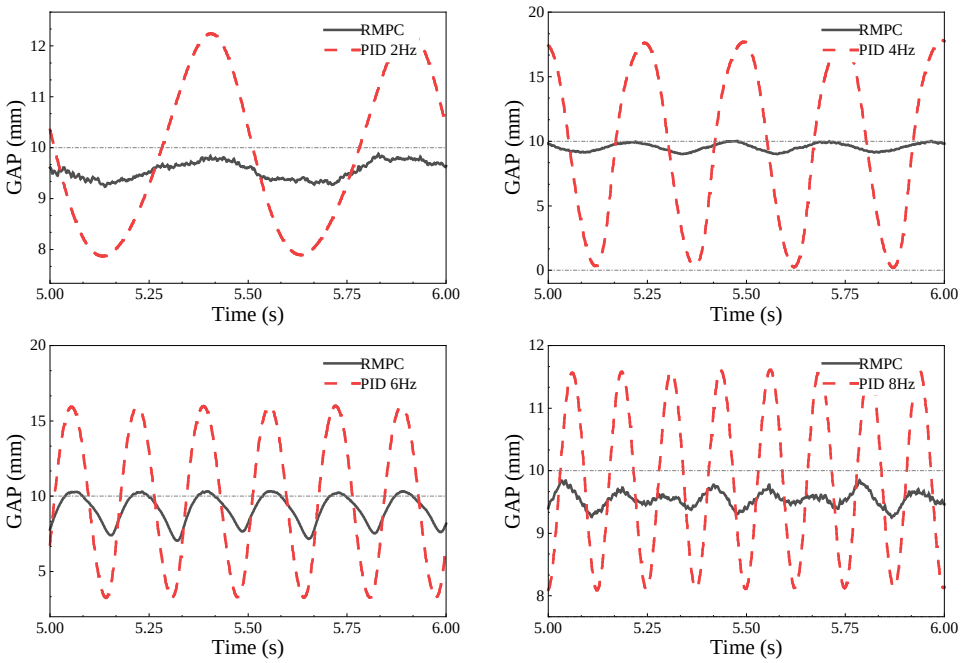

Figure 7 Harmonic aerodynamic load conditions co-simulation results

3.2 Under harmonic track irregularities conditions

The long-wave irregularities due to track joints can significantly affect the stability of a maglev vehicle. The track long-wave irregularities are related to vehicle speed and track length. Using the 50-metre double-span beam of the Shanghai Maglev Demonstration Line as a calculation standard, the track harmonic irregularity excitation is designed for low, medium and high-speed phases:

Group1: $D_{180km/h} = 3mm \cdot \sin\left(2\pi \cdot 2.0t\right)$; Group2: $D_{360km/h} = 3mm \cdot \sin\left(2\pi \cdot 4.0t\right)$; Group3: $D_{603km/h} = 2mm \cdot \sin\left(2\pi \cdot 6.7t\right)$; Group4: $D_{720km/h} = 1mm \cdot \sin\left(2\pi \cdot 8.0t\right)$

Figure 8 shows the levitation gaps under different harmonic track irregularities. From the fluctuation of the gap in the steady state section, it can be seen that the track long-wave irregularities significantly change the suspension stability of the vehicle, and the electromagnet fluctuates around the nominal gap. The fluctuation of the RMPC is smaller than that of the PID. The maximum deviation of the PID is 0.5 mm at 180 km/h, 3.0 mm at 360 km/h, 1.5 mm at 603 km/h, and 1.6 mm at 720 km/h. RMPC can well suppress the vibration in the middle and high-speed stages: the

maximum deviation of 360 km/h is 1.5 mm (50.0% suppression), 603 km/h is 1.3 mm (13.3% suppression), and 720 km/h is 0.9 mm (43.8% suppression). Therefore, RMPC is more robust and anti-interference, which makes it suitable for high-speed magnetic levitation control.

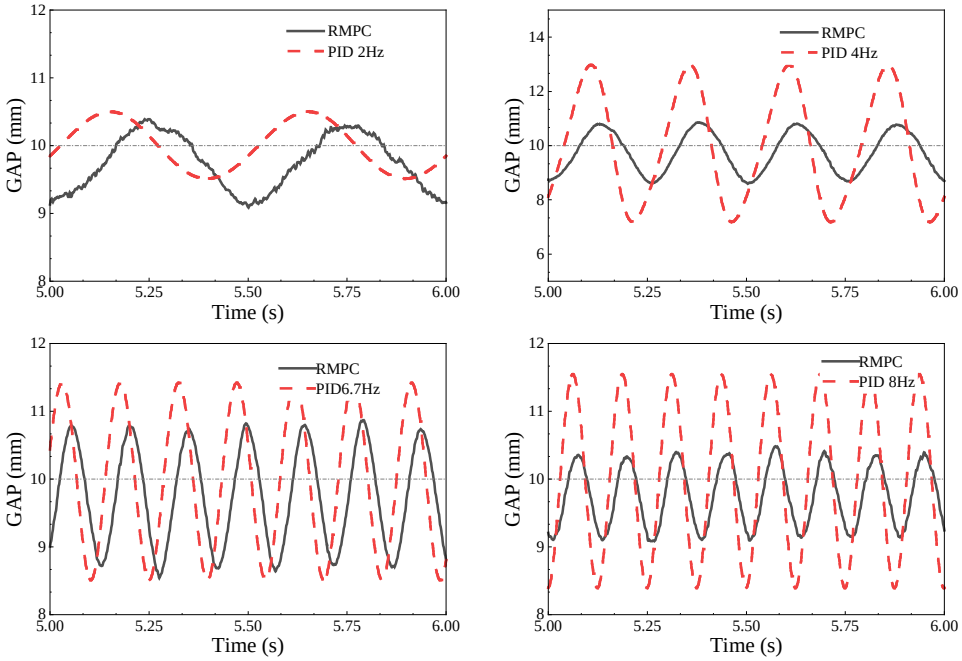

Figure 8 Harmonic track irregularities conditions co-simulation results

3.3 Under non-stationary aerodynamic loads and random track irregularities

In order to verify the robustness of the proposed algorithm, the severe working conditions under the combined effect of random track irregularities and non-stationary aerodynamic loads are tested. ± 2mm random track irregularity is imposed on the system as shown in Figure 9. The designed load is shown in Equation (8). The non-stationary loads and RRBF predictions are shown in Figure 10. The numerical simulation results are displayed in Figure 11.

$$F_r = mg\left[0.30\sin\left(2\pi t\right)+0.22\sin\left(4\pi t\right)+0.14\sin\left(12\pi t+0.5\pi\right)+0.12\sin\left(10\pi t\right)\right] \quad (8)$$

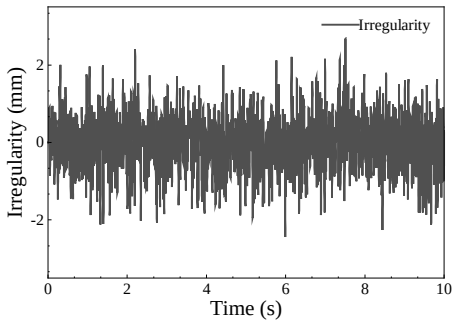

Figure 9 Track vertical irregularity

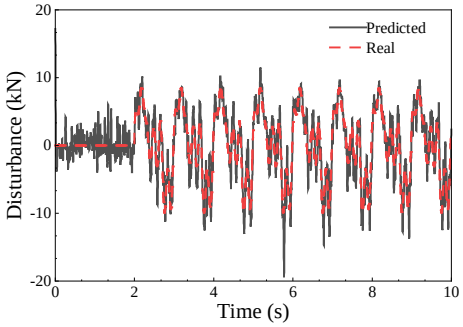

Figure 10 RRBF load prediction

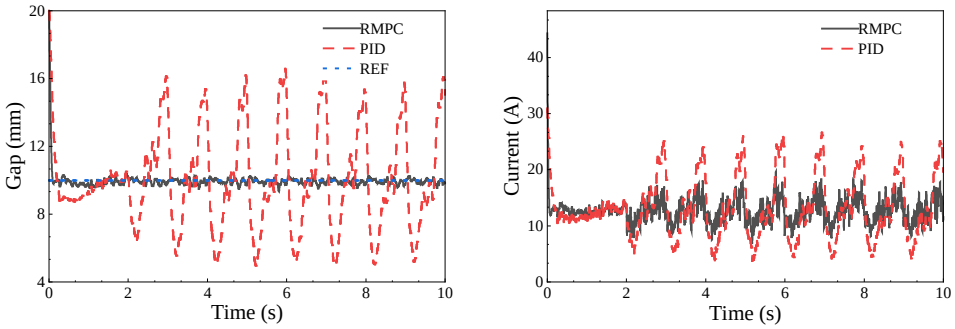

Figure 11 Non-stationary aerodynamic loads and random track irregularities co-simulation results

The electromagnet started levitating from an initial position of 20mm at 0s and levitated to a nominal clearance of 10mm. The track irregularities are loaded synchronously from 0s, and the designed non-stationary aerodynamic loads are applied from 2s. According to Figure 10, the combined effect has an effect on RRBF, and the prediction ability appears to be degraded. But RRBF can still predict the time-varying non-stationary aerodynamic loads. Hence RRBF can correct the prediction model accurately. RMPC can optimize an optimal control sequence based on the dynamic predictive model. The robustness has greatly improved by forwardly counteracting disturbances. In Figure 11, the fluctuations of the electromagnet gap under RMPC control are much smaller than PID's. The maximum gap error for RMPC is 0.67 mm and the maximum gap error for PID is 6.65 mm. Therefore, the proposed RMPC scheme has stronger disturbance suppression capability and robustness.

4 Conclusions

To enhance the anti-interference capabilities of the levitation control system in high-speed operational environments, this paper introduces the Recursive Radial Basis Function Neural Network-based Model Predictive Controller (RMPC). Leveraging the RRBF for aerodynamic load prediction, this innovative approach advances the network's predictive abilities by implicitly incorporating historical information through the structure of local dynamic recursion. The RMPC, an amalgamation of Model Predictive Control (MPC) and RRBF, achieves optimal roll optimization within the finite time domain while adhering to constraints. The foundational Nonlinear Model Predictive Controller (NMPC) adeptly handles the nonlinear characteristics of the Electromagnetic Suspension (EMS) system. Simultaneously, the RRBF excels in forecasting external disturbances in advance. This combined RMPC performs feed-forward compensation for disturbances, effectively suppressing vibrations through rolling optimization. The symbiotic relationship between RRBF and MPC enhances the intelligence of the levitation control algorithm. Conducting extensive numerical studies using the TR08 electromagnet dynamics and control co-simulation model, our findings underscore the remarkable anti-disturbance capabilities of RMPC. Under the joint influence of random track irregularities and high-speed non-stationary aerodynamic loads, RMPC emerges as a superior choice for high-speed magnetic levitation control.

References

[1] ZHAI Wanming, ZHAO Chunfa . Scientific and technological frontiers and challenges of modern rail transit engineering [J]. Journal of Southwest Jiaotong University, 2016,51(2):209-226 .

[2] WANG Zhilu, XU Youlin, LI Guoqiang, et al. Dynamic analysis of a coupled system of high-speed maglev train and curved viaduct [J]. International Journal of Structural Stability and Dynamics, 2018, 18(11): 1-32.

[3] Yau JD (2009) Vibration control of maglev vehicles traveling over a flexible guideway. J Sound Vib 321(1):184–200

[4] SUNG S W, LEE I B, LEE J. Modified proportional-integral derivative (PID) controller and a new tuning method for the PID controller [J]. Ind Eng Chem Res, 2002, 34(11): 4127-4132.

[5] J.H. Lee, Model predictive control: Review of the three decades of development, Int. J. Control Autom. Syst. 9 (2011) 415–424.

[6] M. Ławryńczuk, P. Tatjewski, Offset-free state-space nonlinear predictive control for Wiener systems, Inf. Sci. (Ny) 511 (2020) 127–151, http://dx. doi.org/10.1016/j.ins.2019.09.042.

[7] Shen G, Gang X, Wang H et al (2015) Analysis and experimental study on the MAGLEV vehicle-guideway interaction based on the full-state feedback theory. J Vib Control 21(2):408–416

[8] Sun Y, Qiang H, Mei X et al (2018) Modified repetitive learning control with unidirectional control input for uncertain nonlinear systems. Neural Comput Appl 30(6):2003–2012

[9] Sun, Y., Xu, J., Lin, G. et al. Adaptive neural network control for maglev vehicle systems with time-varying mass and external disturbance. Neural Comput & Applic 35, 12361–12372 (2023).

[10] ZHANG W, WU H, ZENG X, et al. Study of chattering suppression for the sliding mode controller of an electromagnetic levitation system. Journal of Vibration and Control. 2022;0(0).

[11] Zhang Weiwei, Wu Han, Zeng Xiaohui. Development and application of high-speed magnetic levitation vehicle-rail coupling experimental platform [J]. Mechanics in Engineering, 2023,05(31):1-10.

[12] Qiang H, Li W, Sun Y, Liu X (2017) Levitation chassis dynamic analysis and robust position control for maglev vehicles under nonlinear periodic disturbance. J Vibroeng 19(2):1273–1286.

[13] Broomhead DS, Lowe D. Multi-variable functional interpolation and adaptive networks. Complex System 1988;2(2):321–55.

[14] A. Waibel, T. Hanazawa, G. Hinton, K. Shikano and K. Lang, Phoneme recognition using time delay neural network, IEEE Transactions in Acoustics, Speech and Signal Processing 37(3) (1989) 328-339.

[15] M. W. Mak, A learning algorithm for recurrent radial basis function networks, Neural Processing Letters 2(1) (1995) 27-31.

[16] DING S S, YAO S B, CHEN D W. Aerodynamic lift force of high-speed maglev train[J]. Journal of Mechanical Engineering, 2020, 56(8): 228–234.